Effects of plasma spatial profile on conversion efficiency of laser-produced plasma sources for EUV lithography

Ahmed Hassanein
Valeryi Sizyuk
Tatyana Sizyuk
Sivanandan Harilal
Purdue University
School of Nuclear Engineering
400 Central Drive
West Lafayette, Indiana 47907-2017
E-mail: hassanein@purdue.edu

Abstract. Extreme ultraviolet (EUV) lithography devices that use laser-produced plasma (LPP), discharge-produced plasma (DPP), and hybrid devices need to be optimized to achieve sufficient brightness with minimum debris generation to support the throughput requirements of high-volume manufacturing lithography exposure tools with a long lifetime. Source performance, debris mitigation, and reflector system are all critical to efficient EUV collection and component lifetime. Enhanced integrated models continue to be developed using the High Energy Interaction with General Heterogeneous Target Systems (HEIGHTS) computer package to simulate EUV photon emission, debris generation, and transport in both single and multiple laser beam interaction systems with various targets. A new Center for Materials under Extreme Environments (CMUXE) was recently established to benchmark HEIGHTS models for various EUV-related issues. The models being developed and enhanced were used to study the effect of plasma hydrodynamics evolution on the EUV radiation emission for planar and spherical geometry of a tin target and explain the higher conversion efficiency of a planar target in comparison to a spherical target. HEIGHTS can study multiple laser beams, various target geometries, and pre-pulses to optimize EUV photon production. Recent CMUXE and other experimental results are in good agreement with HEIGHTS simulation. [DOI: 10.1117/1.3224901]

Subject terms: extreme ultraviolet (EUV) lithography; laser-produced plasma (LPP); discharge-produced plasma (DPP); photon transport; magnetohydrodynamic (MHD); High Energy Interaction with General Heterogeneous Target Systems (HEIGHTS); Center for Materials under Extreme Environments (CMUXE).

Paper 09023SSR received Feb. 26, 2009; revised manuscript received May 22, 2009; accepted for publication Jun. 2, 2009; published online Oct. 2, 2009.

1 Introduction

Laser-produced plasma (LPP) devices are recently becoming more popular as the source of EUV production for the advanced lithography. Spitzer et al.[1] performed an experimental study of laser irradiation on several materials for generating EUV radiation and showed that tin is one of the most promising target materials for EUV production around 13.5-nm wavelength. The experiment also examined the dependence of the conversion efficiency (CE) on the intensity, wavelength, and pulse width of the laser beam.

Recently, LPP processes for the optimization of EUV production were studied using several target materials (such as xenon, lithium, and tin),[2–4] different target geometry and composition (solid, liquid, cluster grains, etc.),[5,6] and various laser radiation parameters (power density, wavelength, and pulse duration).[7] Numerous experiments and computer simulations were made to increase the EUV radiation power. Such analysis also included the use of pre-pulses for formation of the optimum plasma plume for EUV production during the main laser pulse.[8–10] The optimization of target geometry for efficient laser energy absorption was analyzed using liquid-jets,[11] droplets with tuning of droplet size and laser spot size ratio,[12] and the use of planar targets with various thicknesses.[13] The implementation of mass-limited Sn-doped targets for the production of optically thin plasma and minimization of tin debris was also studied.[13,14] The influence of the spatial plasma effects using multilaser systems for better plasma confinement[15] and the uniformity of spherical target heating by multiple laser beams have indicated potential significant enhancement of EUV production.[16] Recent experimental and theoretical efforts[9,17,18] show the importance of the hydrodynamic effects during plasma evolution on EUV generation. These studies observed an increase in EUV emission near the target surface located close to the laser spot or in the location of the colliding plasma plumes. This effect is believed to be due to the geometrical confinement/containment of motion of the heated plasma, i.e., the density of the hot plasma increases in such locations with an optimum balance of the plasma density/temperature for the EUV production.

Enhanced and integrated models are being developed using the High Energy Interaction with General Heterogeneous Target Systems (HEIGHTS) computer package[15,19,20] to simulate plasma evolution, EUV emission, and debris generation with mitigation/transport in single, multiple, and colliding plasmas. A new Center for Materials under Extreme Environments (CMUXE) was recently established at

1932-5150/2009/$25.00 © 2009 SPIE

Purdue University to benchmark HEIGHTS models against LPP-designed experiments using various Nd:YAG and CO_2 lasers. The models being developed and enhanced include, for example, new ideas and parameters of multiple laser beams in different geometrical configurations and with different pre-pulses to maximize EUV production. Another recent idea being pursued to enhance the production of EUV is to collide two plasma streams together. However, the study of the EUV generation in colliding plasma becomes more difficult because of the complex multidimensional character of the hydrodynamic and radiation transport problem of the two moving plasma streams. Our objective in this study is to use the integrated HEIGHTS package to benchmark recent experiments and to explore ways of maximizing the EUV radiation power.

2 Mathematical and Physical Model

In general, to construct comprehensive and efficient integrated models, the plasma formation and motion is solved using the set of four conservation laws—mass, momentum, energy, and magnetic field—in two-temperature approximation.[18] The final hydrodynamic equation set for LPP devices in matrix form can be described in the following form:

$$\frac{\partial \mathbf{U}}{\partial t}+\frac{1}{r}\frac{\partial}{\partial r}[r\mathbf{F}(\mathbf{U})]+\frac{\partial \mathbf{P}(\mathbf{U})}{\partial r}+\frac{\partial \mathbf{G}(\mathbf{U})}{\partial z}=\mathbf{\Omega}, \tag{1}$$

where the hydrodynamic fluxes are

$$\mathbf{U}=\begin{bmatrix}\rho\\ \rho v^r\\ \rho v^z\\ e_h\\ e_i\end{bmatrix}\quad \mathbf{F}(\mathbf{U})=\begin{bmatrix}\rho v^r\\ \rho v^r v^r\\ \rho v^z v^r\\ v^r(e_h+p_h)\\ v^r(e_i+p_i)\end{bmatrix},$$

$$\mathbf{P}(\mathbf{U})=\begin{bmatrix}0\\ p_h\\ 0\\ 0\\ 0\end{bmatrix}\quad \mathbf{G}(\mathbf{U})=\begin{bmatrix}\rho v^z\\ \rho v^r v^z\\ \rho v^z v^z+p_h\\ v^z(e_h+p_h)\\ v^z(e_i+p_i)\end{bmatrix}, \tag{2}$$

and the dissipative terms are combined in the source $\mathbf{\Omega}$, given as

$$\mathbf{\Omega}=\begin{bmatrix}0\\ 0\\ 0\\ Q_{e,th}+Q_{i,th}+Q_{las}+Q_{rad}\\ Q_{i,th}+Q_{ei}\end{bmatrix}. \tag{3}$$

Here, $Q_{e,th}$ is the electron heat conduction, $Q_{i,th}$ is the ion heat conduction, Q_{rad} is the radiation power, and Q_{ei} is the electron-ion interaction. We use Gaussian units unless indicated otherwise. The conservative form of the initial equations allows the use of the total variation diminishing method in the Lax-Friedrich formulation (TVD-LF)[21] for the solution of the convective stage given by Eq. (1). The numerical scheme for the TVD-LF method applied to the cylindrical symmetry case was described in Ref. 22. Following the splitting method, the Q-terms in Eq. (3) are calculated separately with the second (dissipative) stage of the HEIGHTS solver and are used as correctors for the main TVD-LF solution.[15] An implicit numerical scheme with sparse matrix linear solvers is used for calculating the terms $Q_{e,th}$ and $Q_{i,th}$. (Refs. 19 and 23 The electron-ion interaction term $Q_{ei}=3(m_e n_e/m_i\tau_e)(k_B T_e-k_B T_i)$ is calculated for each hydrodynamic step and used as input in the right side of Eq. (1), where m is the mass; n_e and τ_e are electron concentration and the relaxation time, respectively; e is the electron charge; and k_B is the Boltzmann constant. Detailed description of the HEIGHTS 3-D Monte Carlo radiation transport model is given in Ref. 18.

Ideally, the laser absorption by a target should be treated in two phases: first by the cold, unperturbed solid/liquid target and then by the target having an evolving plasma layer above the remaining solid/liquid target. Most of the hydrodynamics codes developed for infrared, visible, or UV laser interaction consider the plasma creation as instantaneous, at least compared to the driving laser duration. In this approximation, the laser interacts only with the expanding plasma because the beam is reflected at the critical density, which is typically about a hundred times lower than the solid density. In reality, a sharp distinguished boundary does not exist between these two phases. This becomes important because of the complex hydrodynamic flows near the target surfaces, where we should take into account the various energy input from laser radiation, i.e., absorption/reflection in solid/liquid target, absorption/reflection in target vapor, and absorption/reflection in plasma layer. Because the production of the initial EUV radiation area above the target surface consumes part of the laser beam energy and part of main pulse duration, the final efficiency of the LPP device increases with decreasing the time needed for such a preparation stage. This entire process includes gradual decreasing of laser absorption in the cold material and increasing absorption in the hot plasma. It is also important to take into account the reabsorption of laser radiation in the evolving plasma after the reflection from the liquid target surface. For accurate modeling of the previously described processes, we used the available experimental optical properties for laser reflection from liquid tin.[24,25] The reflection coefficient can be derived from this data as

$$k_{ref}=\frac{(n-1)^2+k^2}{(n+1)^2+k^2}, \tag{4}$$

where k and n are real and imaginary parts of the refractive index $\vec{n}=n+ik$. To model laser absorption in vapor material, we used the approximation given in Ref. 26. As shown here, one of the main features of the collision-induced absorption is a quadratic dependence of the absorption coefficient on the density (for our case, this corresponds to the pair collisions) and a weak dependence on the temperature.[27] Based on this model, we calculated the absorption coefficient for the target vapor up to 0.7 eV and fitted the dependence between the experimental data for the liquid target[24,25] and the bremsstrahlung coefficient given by[28]

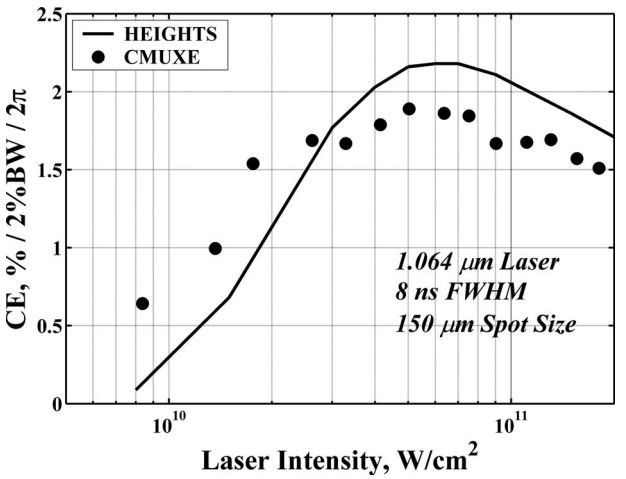

Fig. 1 Dependence of the conversion efficiency on laser intensity both experimentally (CMUXE laboratory) and in computer simulation (HEIGHTS package).

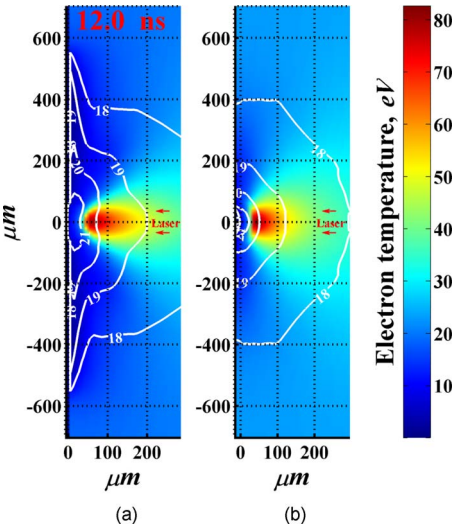

Fig. 2 Electron temperature and density (white contours) distributions in planar (a) and droplet (b) target geometries.

$$k_{abs}^{las} = \frac{16\pi Z n_e^2 e^6 \ln \Lambda(\nu)}{3c\nu^2 (2\pi m_e k_B T_e)^{3/2} (1 - \nu_p^2/\nu^2)^{1/2}}, \tag{5}$$

and to be scaled as

$$k_{abs} \sim \rho^2 T_e^{1/2}, \tag{6}$$

where e, n_e, m_e, T_e are the electron charge, concentration, mass, and temperature, respectively; Z is the normalized ionic charge; ν is the frequency of laser light; $\nu_p = (n_e e^2/\pi m_e)^{1/2}$ is the plasma frequency; k_B is the Boltzmann constant; and ρ is the plasma density. The Coulomb logarithm is given by

$$\ln \Lambda = \ln \left\{ \frac{3}{2} \left[\frac{(k_B T_e)^3}{\pi n_e} \right]^{1/2} \frac{1}{Ze^3} \right\}. \tag{7}$$

3 Modeling Results and Discussion

To study the spatial hydrodynamic effects of spherical and planar targets on the EUV production, we modeled laser interaction with both a tin droplet and a slab target. Similar laser parameters were used in both cases, i.e., 1.064-μm laser wavelength with 70-μm spot size and 8-ns (full width at half maximum) duration. The diameter of the droplet was chosen to be two times larger than the laser spot size to allow efficient utilization of the laser energy, and the target can still be considered as spherical.

We compared the HEIGHTS integrated modeling with the experimental data obtained in our new CMUXE laboratory. Laser beams with 8-ns duration and 150-μm spot size on a planar target were used in both the experiment and for the HEIGHTS simulation. The dependence of the CE on laser beam intensity is shown in Fig. 1 and demonstrates a good agreement with the models in both the magnitudes and the trends.

One of the main goals of this study is to determine the role of the hydrodynamic evolution and confinement processes as the potential cause for the differences in the CE between the planar and spherical targets. HEIGHTS showed that planar targets provide greater geometrical plasma confinement in comparison to the spherical case. This hydrodynamic geometrical confinement prevents the plasma from quickly escaping from the EUV production zone. Figure 2 shows the electron temperature and density distributions at 4 ns after the peak of the laser beam with an intensity of 5×10^{11} W/cm^2 (FWHM) irradiated the target surface. The target surface is located in all cases near the zero point. The plasma near the target surface with electron density of around 10^{20} cm^{-3} and electron temperature of $\sim$30 eV forms the most productive EUV radiation area for these conditions. As shown in Fig. 3, a significant part of the emitted photons is absorbed around this area in the denser zone (close to the target surface) or in the more hot areas. The EUV radiation fluxes have larger values in surrounding regions.

The HEIGHTS Monte Carlo model for radiation transport simulation permits us to determine the location and intensity of the photon source for EUV output in 2π sr

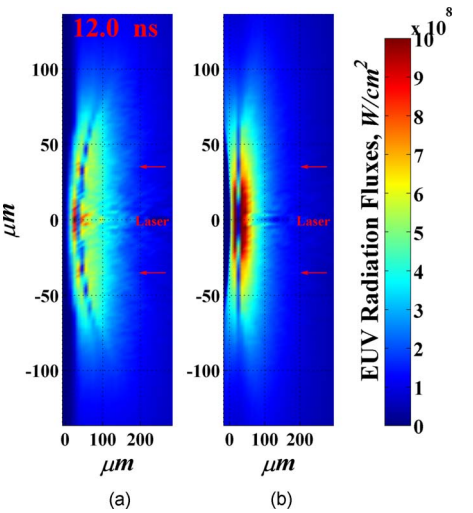

Fig. 3 Radiation fluxes in the EUV range for planar (a) and droplet (b) target geometries.

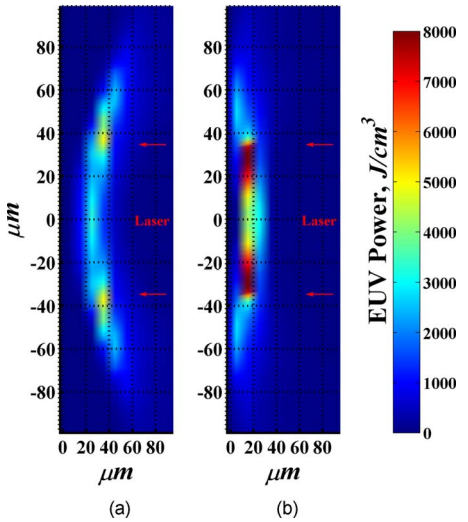

Fig. 4 Location and intensity of the EUV power collected during 20 ns in 2π sr in planar (a) and droplet (b) target geometries.

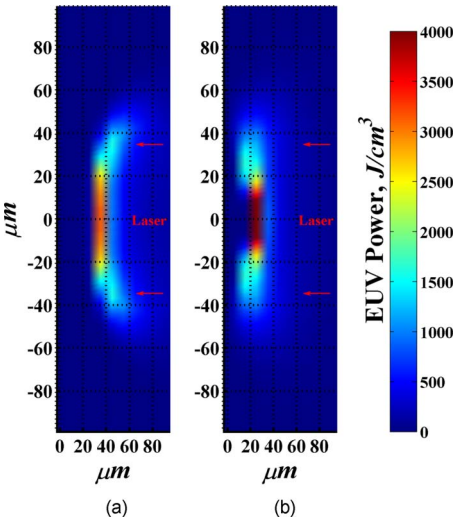

Fig. 6 Location and intensity of the collected EUV power during 20 ns in 2π sr in planar (a) and droplet (b) target geometries.

(Fig. 4). The shape of the EUV source area corresponds to the shape of the optimum plasma plume for photon production and depends on the area of the absorbing plasma. Figure 4 illustrates the source of EUV photons collected during 20 ns with laser pulse width 8 ns (FWHM).

As shown earlier, Figs. 2–4 correspond to an intense laser heating of 5×10^{11} W/cm^2. This analysis shows that the effective plasma confinement in the case of high laser energy input causes the plasma to overheat and therefore decreases the CE. Figure 5 confirms this observation. The planar target is more effective than the droplet target for small and medium laser radiation intensities. The overheating reverses this situation for laser intensities higher than $\sim2.5\times10^{11}$ W/cm^2.

At lower laser intensities, the plasma is not excessively overheated and the size of EUV area is larger for the planar geometry because of better plasma evolution and containment. The EUV radiation area produced by laser heating of intensity 7×10^{10} W/cm^2 is shown in Fig. 6. The most significant EUV photon production zone is located around the spot center, in contrast to the previously described situation. At higher laser intensities, hydrodynamic plasma evolution moving away from the area of laser energy deposition/absorption prevents further plasma overheating in the system with the spherical configuration (Fig. 4). Therefore, the difference in CE for planar and spherical targets can be explained by the nature of hydrodynamic geometrical containment. Conditions for high plasma density with stable optimum temperature should be created to obtain the highest CE. The plasma temperature stability is provided by the balance between the incoming and escaping energy, i.e., laser energy absorption, radiation energy loss, and plasma expansion. The last term is mainly controlled by hydrodynamic and geometrical confinement.

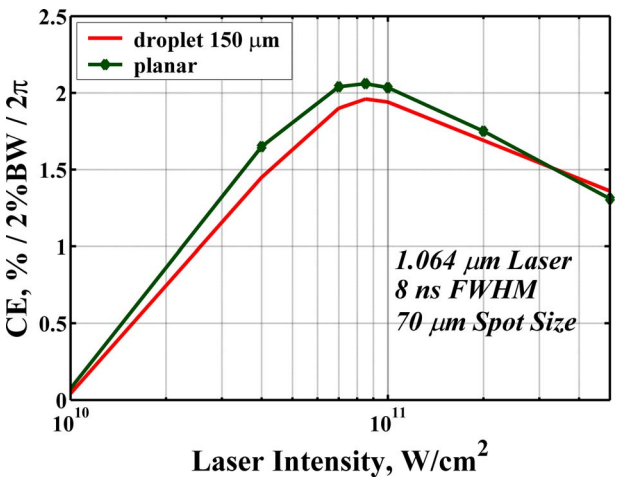

Fig. 5 Dependence of the conversion efficiency on laser intensity for both sphere and planar geometries.

These geometrical hydrodynamic effects control the plasma motion, i.e., limit and control the escaping plasma from the laser heating area and from the most productive EUV generation zone. In the case of the larger laser heating region, lower laser intensities are needed to create the efficient EUV production area because of the longer time of the plasma motion under the laser beam. The smaller laser irradiation spots produce opposite effects. As a result, the hydrodynamic confinement is believed to be the cause of the right shift of the maximum CE due to the decrease of the laser beam radius (see Fig. 7). This is a consequence of the hydrodynamic evolution where the plasma confinement can play an important role. The main effects to maximize EUV production are to create the right plasma density and temperature conditions with maximum size for the longest possible period of time.

4 Conclusion

Enhanced integrated hydrodynamic, plasma, and photon transport models continue to be developed and implemented in the HEIGHTS computer package to simulate EUV emission in both laser- and discharge-produced plasma devices. The developed and enhanced models were used to analyze the influence of spatial hydrodynamic plasma evolution on the EUV radiation generation for pla-

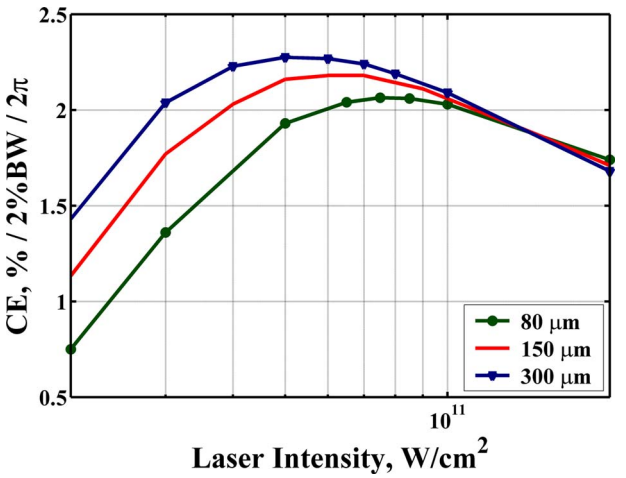

Fig. 7 Dependence of the conversion efficiency on laser intensity and beam spot size.

nar and spherical geometries of a tin target in LPP devices. The higher efficiency of a planar target in comparison to spherical geometry was explained due to better hydrodynamic geometrical containment of the heated plasma. A new Center for Materials under Extreme Environments (CMUXE) laboratory was recently established to conduct LPP experiments to benchmark HEIGHTS models for EUV photon production and the study of plasma debris effects on collector mirror reflectivity. Recent CMUXE experimental results for plasma production and laser conversion efficiency agree well with the HEIGHTS models.

References

1. R. C. Spitzer, T. J. Orzechowski, D. W. Phillion, R. L. Kauffman, and C. Cerjan, "Conversion efficiencies from laser-produced plasmas in the extreme ultraviolet regime," *J. Appl. Phys.* **79**(5), 2251–2258 (1996).
2. H. Shields, S. W. Fornaca, M. B. Petach, M. Michaelian, D. R. Mcgregor, R. H. Moyer, and R. J. St. Pierre, "Xenon target performance characteristics for laser-produced plasma EUV sources," *Proc. SPIE* **4688**, 94–101 (2002).
3. G. O'Sullivan, A. Cummings, P. Dunne, P. Hayden, L. McKinney, N. Murphy, and J. White, "Atomic physics of highly charged ions and the case for Sn as a source material," Chapter 5 in *EUV Source for Lithography*, V. Bakshi, Ed., pp, 149–173, SPIE press, Bellingham, WA (2006).
4. P.-E. Nica, S. Miyamoto, S. Amano, T. Inoue, A. Shimoura, K. Kaku, and T. Mochizuki, "Soft x-ray spectra from laser heated lithium targets," *Appl. Phys. Lett.* **89**, 041501 (2006).
5. T. Abe, T. Suganuma, Y. Imai, Y. Sugimoto, H. Someya, H. Hoshino, G. Soumagne, H. Komori, H. Mizoguchi, A. Endo, and K. Toyoda, "Development of liquid-jet laser-produced plasma light source for EUV lithography," *Proc. SPIE* **5037**, 776–783 (2003).
6. K. Nagai, Q. Gu, T. Norimatsu, S. Fujioka, H. Nishimura, N. Miyanaga, K. Nishihara, Y. Izawa, and K. Mima, "Nano-structured lithium-tin plane fabrication for laser produced plasma and extreme ultraviolet generation," *Laser Part. Beams* **26**, 497–501 (2008).
7. T. Nishikawa, A. Sunahara, A. Sasaki, and K. Nishihara, "EUV source design flexibility for lithography," *J. Phys.: Conf. Ser.* **112**, 042065 (2008).
8. S. Dusterer, H. Schwoerer, W. Ziegler, D. Salzmann, and R. Sauerbrey, "Effects of a prepulse on laser-induced EUV radiation conversion efficiency," *Appl. Phys. B* **76**, 17–21 (2003).
9. R. de Bruijn, K. N. Koshelev, S. V. Zakharov, V. G. Novikov, and F. Bijkerk, "Enhancement of laser plasma extreme ultraviolet emission by shockwave-plasma interaction," *Phys. Plasmas* **12**, 042701 (2005).
10. L. R. Hoffman, A. N. Bykanov, O. V. Khodykin, A. I. Ershov, N. R. Bowering, I. V. Fomenkov, W. N. Partlo, and D. W. Myers, "LPP EUV conversion efficiency optimization," *Proc. SPIE* **5751**, 892–901 (2005).
11. B. A. M. Hansson and H. M. Hertz, "Liquid-jet laser-plasma extreme ultraviolet sources: from droplets to filaments," *J. Phys. D: Appl. Phys.* **37**, 3233–3243 (2004).
12. S. Yuspeh, K. L. Sequoia, Y. Tao, M. S. Tillack, R. Burdt, and F. Najmabadi, "Optimization of the size ratio of Sn sphere and laser focal spot for an extreme ultraviolet light source," *Appl. Phys. Lett.* **93**, 221503 (2008).
13. S. Fujioka, H. Nishimura, T. Okuno, Y. Tao, N. Ueda, T. Ando, H. Kurayama, Y. Yasuda, Y. Shimada, M. Yamaura, Q. Gu, K. Nagai, T. Norimatsu, H. Furukawa, A. Sunahara, Y.G. Kang, M. Murakami, K. Nishihara, N. Miyanaga, and Y. Izawa, "Properties of EUV and particle generations from laser-irradiated solid- and low-density tin targets," *Proc. SPIE* **5751**, 578–587 (2005).
14. P. Hayden, A. Cummings, N. Murphy, G. O'Sullivan, P. Sheridan, J. White, and P. Dunne, "13.5-nm extreme ultraviolet emission from tin-based laser-produced plasma sources," *J. Appl. Phys.* **99**, 093302 (2006).
15. V. Sizyuk, A. Hassanein, and T. Sizyuk, "Three-dimensional simulation of laser-produced plasma for extreme ultraviolet lithography applications," *J. Appl. Phys.* **100**, 103106 (2006).
16. Y. Shimada, H. Nishimura, M. Nakai, K. Hashimoto, M. Yamaura, Y. Tao, K. Shigemory, T. Okuno, K. Nishihara, T. Kawamura, A. Sunahara, T. Nishikawa, A. Sasaki, K. Nagai, T. Norimatsu, S. Fujioka, S. Uchida, N. Miyanaga, Y. Izawa, and C. Yamanaka, "Characterization of extreme ultraviolet emission from laser-produced spherical tin plasma generated with multiple laser beams," *Appl. Phys. Lett.* **86**, 051501 (2005).
17. M. S. Tillack, K. L. Sequoia, and Y. Tao, "Geometric effects on EUV emissions in spherical and planar targets," *J. Phys.: Conf. Ser.* **112**, 042060 (2008).
18. V. Sizyuk, A. Hassanein, and T. Sizyuk, "Hollow laser self-confined plasma for extreme ultraviolet lithography and other applications," *Laser Part. Beams* **25**, 143–154 (2007).
19. V. Sizyuk, A. Hassanein, V. Morozov, V. Tolkach, and T. Sizyuk, "Numerical simulation of laser-produced plasma devices for EUV lithography using the heights integrated model," *Numer. Heat Transfer, Part A* **49**, 215–236 (2006).
20. V. Sizyuk, A. Hassanein, V. Morozov, and T. Sizyuk, "HEIGHTS integrated model as instrument for simulation of hydrodynamic, radiation transport, and heat conduction phenomena of laser-produced plasma in EUV applications," Report ANL-MCS-CPH-06/56, Argonne National Laboratory (2006).
21. R. J. Leveque, *Finite Volume Methods for Hyperbolic Problems*, Cambridge University Press, Cambridge, UK (2002).
22. A. Hassanein, V. Sizyuk, V. Tolkach, V. Morozov, and B. J. Rice, "HEIGHTS initial simulation of discharge-produced plasma hydrodynamics and radiation transport for extreme ultraviolet lithography," *J. Microlithogr., Microfabr., Microsyst.* **3**, 130–138 (2004).
23. G. V. Miloshevsky, V. A. Sizyuk, M. B. Partenskii, A. Hassanein, and P. C. Jordan, "Application of finite-difference methods to membrane-mediated protein interactions and to heat and magnetic field diffusion in plasmas," *J. Comp. Physiol.* **212**, 25–51 (2006).
24. J. P. Petrakian, A. R. Cathers, J. E. Parks, R. A. MacRae, T. A. Callcott, and E. T. Arakawa, "Optical properties of liquid tin between 0.62 and 3.7 eV," *Phys. Rev. B* **21**, 3043–3046 (1980).
25. G. Cisneros, J. S. Helman, and C. N. J. Wagner, "Dielectric function of liquid tin between 250 and 1100 °C," *Phys. Rev. B* **25**, 4248–4251 (1982).
26. G. G. Grigoryan, A. G. Leonov, E. A. Manykin, A. A. Rudenko, M. G. Sitnikov, and A. N. Starostin, "The near infrared (0.8–2.6 μm) absorption spectrum of a dense sodium vapor and possible mechanisms of the spectrum formation," *JETP* **97**, 678–687 (2003).
27. L. Frommhold, *Collisional-Induced Absorption in Gases*, Cambridge University Press, Cambridge, UK (1993).
28. T. W. Johnston and J. M. Dawson, "Correct values for high-frequency power absorption by inverse Bremsstrahlung in plasmas," *Phys. Fluids* **16**, 722 (1973).

Ahmed Hassanein is Paul L. Wattelet Professor and Head of Nuclear Engineering at Purdue University. He received BS and MS degrees in nuclear engineering from Alexandria University, Egypt. two MS degrees — in nuclear engineering and physics from the University of Wisconsin-Madison, and his PhD in nuclear engineering fro the University of Wisconsin-Madison. he has more than 25 years of experience in research and development in nuclear engineering, physics, and material science fields. Dr. Hassanein is the author of more than 350 journal publications and technical reports in more than 18 different journals in many fundamental sience areas including heat

transfer, thermal hydraulics, radiation damage and materials' lifetime, hydrodynamics, particle diffusion and transport, atomic and plasma physics, photon and radiation transport, laser and discharge produced plasmas, nanotechnology, and biomedical.

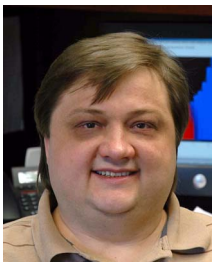

Valeryi Sizyuk is a research Assistant Professor at Purdue Univeristy, West Lafayette, IN. He received his PhD in physics and mathematics in 1997 in Belarus State University, Minsk. His major research areas include magnetohydrodynamics, thermal heat conduction, radiation transport processes in plasma. Other fields of interest include numerical methods for calculations, Monte Carlo algorithms, parallel programming, and software developments. He has been a member of the HEIGHTS team since 2002.

Tatyana Sizyuk is a computer analyst and researcher at Purdue University. She received her BS and MS degrees in applied mathematics from Belarus State University, Minsk. She is experienced in computer programming and code development (FORTRAN and C), parallel programming (MPI), graphical post processing (MATLAB), graphical applications for multiplatform software (OpenGL, GLUT, and GTK), PC cluster organization for parallel calculations, parallel simulations on computer clusters (350–node ANL Jazz cluster) and IBM BG/L and BG/P computer systems.

Sivanandan Harilal is a research Assistant Professor at Purdue Univeristy, West Lafayette, IN. He received his PhD from Cochin University of Science and Technology, India in 1998. He was awarded the Alexander von Humboldt Fellowship immediately after receiving doctorate degree and joined with Professor H. J. Kunze's group at Ruhr Univeristat in Bochum, Germany. Dr. Harilal also served at various academic and scientific prositions at University of California San Diego, Argonne National Laboratory and Prism Computational Science, Inc. In 2009 Dr. Harilal joined the School of Nuclear Engineering faculty at Purdue University. He has co-authored more than 70 scientific journal articles and book chapters in the fields of laser-produced plasma applications, LIBS, plasma diagnostics and plasma-facing components.